Available online at www.eccomasproceedia.org
Eccomas Proceedia COMPDYN (2017) 3406-3425

ECCOMAS
Proceedia

compdybCOMPDYN 2017
6th ECCOMAS Thematic Conference on
Computational Methods in Structural Dynamics and Earthquake Engineering
M. Papadrakakis, M. Fragiadakis (eds.)
Rhodes Island, Greece, 15–17 June 2017

IN-PLANE SEISMIC PERFORMANCE OF RC STRUCTURES WITH AN INNOVATIVE MASONRY INFILL WITH SLIDING JOINTS THROUGH NON-LINEAR ANALYSES

A. Rossi[1], P. Morandi[2], R.R. Milanesi[2], and G. Magenes[1,2]

[1] IUSS Pavia
Piazza della Vittoria 15, Pavia, Italy
andrea.rossi@iusspavia.it

[2] Dep. of Civil Engineering and Architecture of the University of Pavia and EUCENTRE
Via Ferrata 1/3, Pavia, Italy
paolo.morandi@unipv.it
riccardo.milanesi@unipv.it
guido.magenes@unipv.it

Keywords: Innovative infill with sliding joints, in-plane seismic response, performance levels, macro-modelling, non-linear analyses on infilled structures.

Abstract. *Within the European FP7 Project "INSYSME", the research unit of the University of Pavia has conceived a new seismic resistant masonry infill system with sliding joints, which allows in-plane damage control of the masonry and the reduction of the detrimental effects due to the panel-frame interaction. The system proposed ([1] and [2]) has been subjected to an extensive experimental campaign and both the in-plane and out-of-plane seismic behaviour of RC frames with the innovative infills with and without opening have been examined ([3] and [4]) In this paper, a study on the in-plane seismic performance of RC structures with the newly developed infills has been conducted through nonlinear static and dynamic analyses. The experimental cyclic in-plane response has been calibrated through numerical simulations of the tests by representing the masonry infill as two compressive diagonal struts pinned at its ends to the intersection of beam and column centrelines. Nonlinear analyses on 6-storey 3-bay RC frames designed for different levels of PGA have been conducted. Bare and infilled frames have been taken into account and various infilled configurations have been considered, also examining the case with and without openings. The results have permitted to study the influence of the infill on the global in-plane behaviour of the structure, in particular in terms of displacement and inter-storey drift demands and their reduction as respect to bare configurations. The definition of specific performance levels at the infill level according to the amount of damage attained in the cyclic in-plane tests ([3] and [4]), has allowed determining a consistent criterion for the attainment of the limit state conditions at the level of the building, considering the actual performance of the infills in the structures in terms of the drift demand versus capacity. Finally, a comparison between the results of the non-linear analyses on the structural configurations infilled with the innovative solution and with a "traditional" infill typology (double-leaf masonry in adherence at the RC structure [7]) has been performed, clearly highlighting the improvement of the in-plane seismic response of the newly developed system.*

Peer-review under responsibility of the organizing committee of COMPDYN 2017.
doi: 10.7712/120117.5654.18698

1 INTRODUCTION

Since more than fifty years, many researchers have studied the seismic behavior of masonry infills and analyzed their interaction with the surrounding RC frame structures. A large amount of experimental tests and numerical analyses has been carried out with the aim of reducing the vulnerability of masonry infills subjected to seismic actions. The main goal of these studies is to find a cost-effective technological solution able to limit the damage in the infills and guarantee their lateral stability, while the thermal, acoustic and durability performances are not compromised.

In accordance with the "traditional" construction solution, masonry infills and the surrounding RC frames are completely in contact. The infills are usually built after the casting and hardening of the RC frame, and no gaps or any particular connections are inserted in between these elements. The traditional masonry infill solution has a series of critical aspects, related to both in-plane and out-of-plane seismic response, pointed out by the outcomes of several experimental tests and by the experience in post-seismic surveys [2].

In order to improve the seismic response of the infills and to control the damage and the stability of the panels, the research unit of University of Pavia, within the European FP7 Project "INSYSME" [5], has conceived a new seismic resistant masonry infill system with sliding joints within the wall and flexible joints around the wall-frame interface. The sliding joints divide the infill into horizontal stripes and are designed specifically to allow the relative in-plane movement of these stripes. The detrimental interaction of the infill with the surrounding RC frame is limited by the flexible joints, avoiding the direct impact of the infill against the frame and absorbing part of the energy generated during the shake. Therefore, the local stress concentration in the joints is limited by both the flexible joints at the wall-frame interface and the sliding joints. The out-of-plane stability of the infill is ensured by properly designed "shear keys" attached to the column. Figure 1a shows the details of the innovative masonry infills proposed by University of Pavia and Figure 1b shows the sketch of the in-plane deformed infilled frame; an exhaustive description of the system is reported in Morandi et al. in [1] and [2].

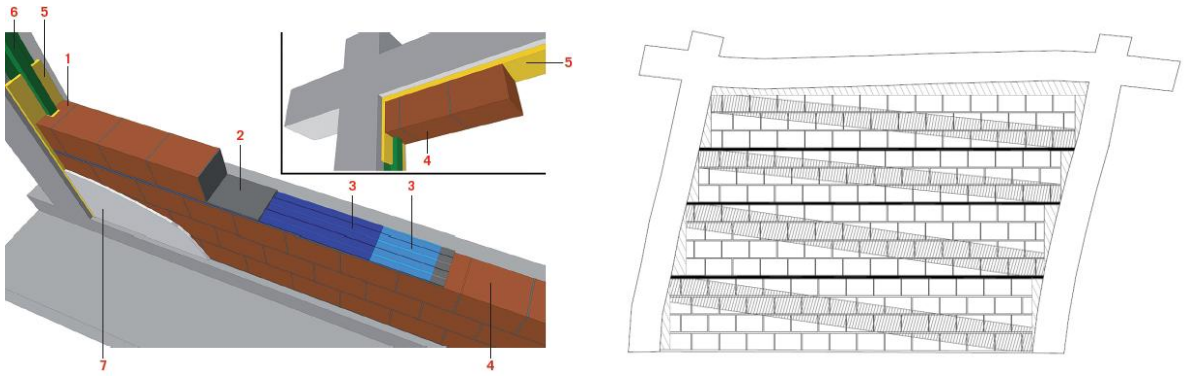

(a) (b)

Figure 1: (a) Details of the innovative masonry infill with sliding joints: 1.C-shape units; 2. mortar bed-joints; 3. Sliding joints; 4. clay units; 5. interface joints; 6. shear keys; 7. Plaster. (b) Sketch of the compressive struts and the deformed frame with the infill with sliding joints

The main objective of this work is to study the in-plane performance of the innovative infill system and its influence in the overall seismic response of RC buildings, also in comparison with the results on a traditional infill solution constituted by a double-leaf wall of horizontally perforated weak clay units.

A series of numerical non-linear static and dynamic analyses were performed on different types of newly designed RC plane frame structures, considering two typologies of innovative infills (with and without opening) and the traditional one without opening, in various infill configurations. A macro-modelling approach was adopted, since the focus of this work is the damage on infills, which is governed essentially by inter-storey drift, and since the large amount of non-linear analyses require a high computational burden; this simplified approach was considered the best solution giving reliable results within reasonable time. The software adopted to perform the non-linear analyses is Ruaumoko2D, a finite element program specifically for non-linear static and dynamic analysis ([6]).

A proper calibration of the numerical macro-model of the innovative infill system proposed by University of Pavia was possible thanks to the results of the experimental tests performed on this infill typology within the European FP7 Project "INSYSME", reported in Milanesi et al. ([3]) and Morandi et al. ([4]).

2 CASE STUDIES

The in-plane cyclic experimental response of the innovative infill system was evaluated by means of in-plane static cyclic tests, within an extensive test campaign executed at the University of Pavia within the European FP7 Project ([5]).

Three full-scale specimens were tested in-plane: a single story - single bay RC bare frame called “TNT”), a fully infilled frame (“TSJ1”) and a partially infilled RC frame with a 1.42 m wide central opening at the entire height (“TSJ2”). The geometry of the RC frame surrounding the innovative infills was the same for the three frames. The concrete class was C28/35 and the steel adopted for the steel reinforcement was of type B450C. The masonry was made up by vertically hollowed plain clay units (length x height x thickness = 30 x 19 x 25 cm) and general-purpose mortar, being the overall thickness of the wall equal to 29 cm (25 cm thick units with 2 cm thick plaster at both sides). Figure 2 shows a schematic representation of the three tested specimens along with the reinforcement details of the RC frames.

In addition to the innovative infills, a traditional infill system, constituted by a double-leaf wall of horizontally perforated weak clay units (length x height x thickness = 25 x 25 x 12 cm) cast in complete adherence to the RC frame (see Figure 3) has been taken into account to establish a comparison with a commonly adopted infill typology. This masonry infill (called “T2”) has been suitably calibrated by Hak et al. ([7]), on in-plane cyclic tests carried out by Calvi and Bolognini ([8]).

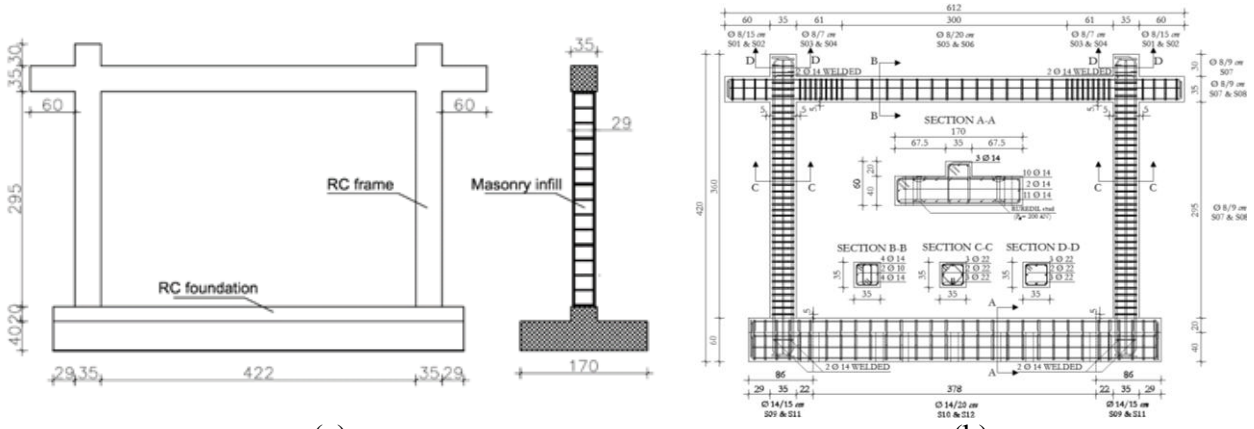

(a) (b)

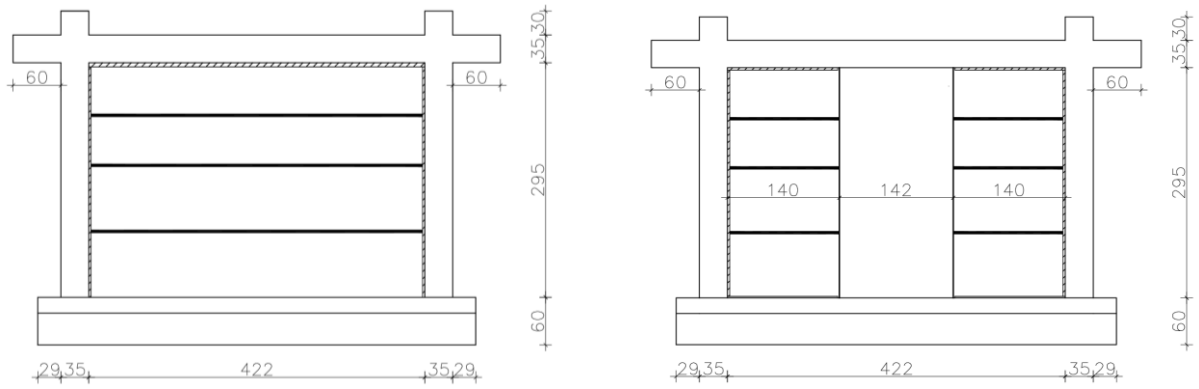

Figure 2: Frame configurations: a) RC bare frame (TNT); b) reinforcement details of the RC frame; fully infilled frame (TSJ1); d) partially infilled frame (TSJ2).

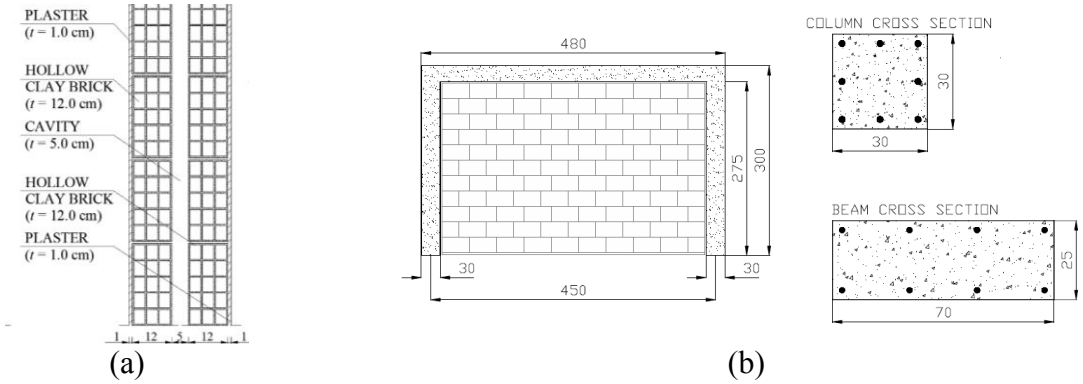

Figure 3: (a) "Traditional" infill type: vertical section of the double-leaf wall [7]; (b) Geometry of the frames tested by Calvi and Bolognini [8]

In order to evaluate the influence of the infills in terms of overall in-plane response of RC buildings, six-storey RC frame structures were chosen to be representative of typical infilled buildings in the European context. The height of each storey was 3.0 m and the building was composed by four RC plane frames internally spaced of 5.0 m, each of them consisting of three bays of 5.0 m, 2.0 m and 5.0 m, respectively. The case study selected to be analyzed is the internal plane frame shown in Figure 4. The materials used for the building are concrete of class C28/35 and reinforcement steel of class B450C.

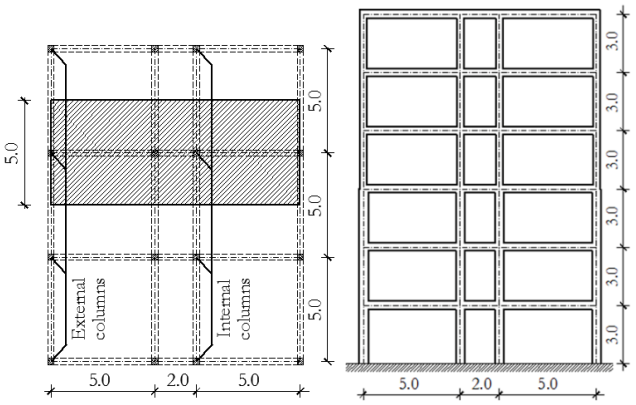

Figure 4: Plan and elevation of two-dimensional prototype structure.

The building was designed according to Eurocode 2 [9], Eurocode 8 [10] and NTC 2008 [11], with reference to the results of multimodal dynamic response spectrum analyses performed on linear bare frame models. The elastic gross stiffness of RC elements was reduced of 50% to account for the effect of cracking. The buildings were designed for three levels of seismicity, having a peak ground acceleration on ground type A, a_g, equal to 0.10g, 0.25g and 0.35g and founded on ground type B (a_g was multiplied by the soil factor S, equal to 1.35 for a_g=0.10g and S=1.2 in the other two cases). The ductility class of the building was "high" (DCH) and, in accordance with the code recommendation, the behavior factor of this regular structure, q, was equal to 5.85. The parameters of the elastic and design spectra at the Ultimate Limit State for each of the three values of PGA have been selected according to Eurocode 8 [10] (response spectrum Type 2 has been adopted for the seismicity level with a_g of 0.10g, response spectrum Type 1 has been used for the other two cases). The members of RC frames were dimensioned following the design capacity principles with strong columns and weak beams, in order to avoid "shear failure". The dimensions and the longitudinal reinforcement of the two-dimensional case-study frames are shown in Table 1, Table 2 and Table 3. The two structures designed for a PGA of 0.10g·S and 0.25g·S resulted to be the same, due to the geometry and steel reinforcement minimum requirements given by the codes. Further design details are discussed in Hak et al. in [7].

a_g	**Storey**	**Cross sectional width/height [*cm*]**	
0.10 g – 0.25 g	1st - 3rd	45/45	Columns
	4th – 6th	35/35	
0.35 g	1st - 3rd	55/55	
	4th – 6th	45/45	
0.10 g – 0.25 g – 0.35 g	1st – 6th	30/45	Beams

Table 1: Dimensions of the beams and the columns of the RC frame.

Storey	**a_g =0.10 g - 0.25 g**		**a_g =0.35 g**	
	Exterior column	Interior column	Exterior column	Interior column
1st- 3rd	8 Φ18	8 Φ18	12 Φ18	12 Φ18
4th- 6th	8 Φ18	12 Φ18	8 Φ18	12 Φ18

Table 2: Longitudinal reinforcement of the columns.

Storey	**a_g =0.10 g - 0.25 g**				**a_g =0.35 g**			
	Exterior beam		Interior beam		Exterior beam		Interior beam	
	Top	Bottom	Top	Bottom	Top	Bottom	Top	Bottom
1st- 2nd	4 Φ18	2 Φ18	3 Φ18	2 Φ18	4 Φ18	2 Φ18	4 Φ18	3 Φ18
3rd- 4th	4 Φ18	2 Φ18	2 Φ18	2 Φ18	4 Φ18	2 Φ18	3 Φ18	2 Φ18
5th	4 Φ18	2 Φ18	2 Φ18	2 Φ18	4 Φ18	2 Φ18	2 Φ18	2 Φ18
6th	3 Φ18	2 Φ18	2 Φ18	2 Φ18	3 Φ18	2 Φ18	2 Φ18	2 Φ18

Table 3: Longitudinal reinforcement of the beams.

3 MASONRY INFILLS SEISMIC PERFORMANCES

As better specify in Hak et al. [7], different limit states can be evaluated in terms of drift attained to a correspondent level of damage derived from in-plane cyclic tests on infills. An operational limit state (OLS), a damage limit state (DLS) and a life safety limit state (LSS or ULS) are defined specifically for infill performance. At OLS the infill is considered undamaged or slightly damaged, at DLS the infill is damaged, but can be effectively and economi-

cally repaired, whereas at LSS/ULS the infill is considered severely damaged and reparability is economically questionable, but lives are not threatened.

In Table 4, the in-plane drift capacity corresponding to the different limits states for each infill system has been reported, as defined by Morandi et al. [4] for the innovative infills and by Hak et al. [7] for the traditional double-leaf infill.

LIMIT STATE	Solid infill – Sliding joints TSJ1	Infill with opening - Sliding joints TSJ2	Traditional Infill - Double leaf T2
Drift OLS	0.50%	0.40%	0.20%
Drift DLS	3.00%	0.90%	0.30%
Drift LSS or ULS	> 3.00%	> 3.00%	1.00%

Table 4: Drift limit states of the considered infills ([4], [7]).

4 NUMERICAL CALIBRATION

The numerical-macro models representing the innovative infills were calibrated taking, as reference, the in-plane cyclic tests carried out at the University of Pavia. The results of the in-plane cyclic tests were more largely reported by Morandi et al. ([4]), along with the mechanical properties of the materials obtained from tests of characterization. The in-plane tests were conducted applying a displacement-controlled loading history at increasing drift levels up to very large values, with three reverse cycles performed for each target displacement. The results of the experimental tests were compared to the response of the numerical macro-models in terms of force-displacement curves for the entire displacement history.

The purpose of the calibration was to reproduce numerically the in-plane experimental behavior of the frames with the innovative infill systems, which it was, in turn, necessary to obtain reliable models to be used in the subsequent non-linear analyses at the "building scale".

The infilled frames were modelled using a macro-element approach, using Ruaumoko2D program ([6]). Three models, the simple bare-frame portal, the fully infilled and the one with the central opening, were defined as reported in Figure 5.

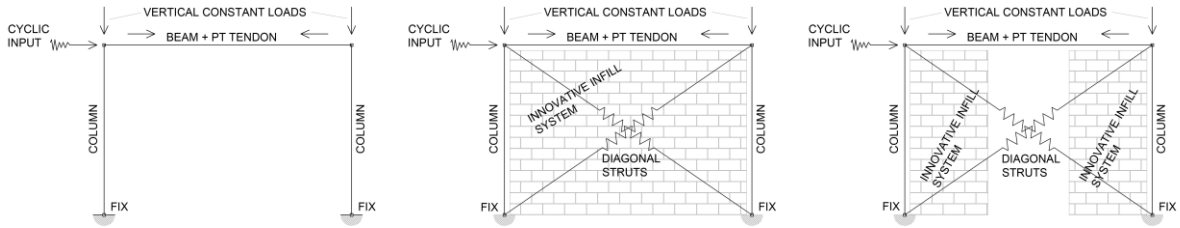

Figure 5: Scheme of the three in-plane cyclic tested specimens.

In the structural models, the RC members of the frames were defined as one-component Giberson elements ([12]) with concentrated plasticity at their ends. Assuming that the design of the frame was properly performed, the possibility of shear failures in the structural members was not taken into account. In accordance with the recommendations of Pristley et al. in [13], the region of intersection between the beam and the columns were characterized by perfectly elastic short elements. The hysteresis rule adopted to simulate the RC behavior of the section of the columns was the Schoettler-Restrepo rule ([6]), while the non-linear behavior of the beam was defined by the Fukada rule ([14]), as shown in Figure 6.

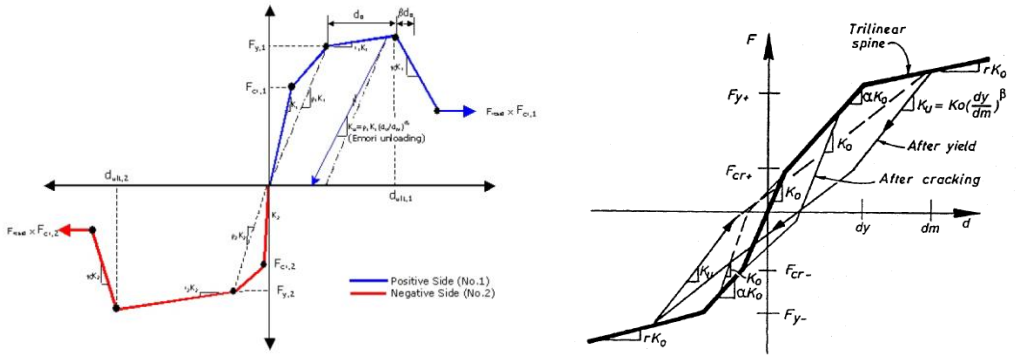

Figure 6: (a) Backbone curve of Schoettler-Restrepo rule [6]; (b) Fukada degrading Tri-linear hysteresis rule [14]

Considering the infilled frame cases, two diagonal non-linear springs that represent the innovative infill system have been considered. These elements were pinned to the extreme nodes of the frame and work only in compression ("no tension" elements). The hysteresis rule associated to the non-linear behaviour of the two diagonal struts representing the infills was the one proposed by Crisafulli in [15], as reported in Figure 7. The innovative infill with the opening was modelled following the same principles of the fully infill. According to the experimental results, the two diagonal spring defined by the Crisafulli hysteresis rule was capable to represent both the configurations of the innovative system, with and without opening.

The springs elements, defined by the Crisafulli hysteresis rule, are defined by an elastic modulus (E_{mo}), a compressive strength (f'_m) and an initial stiffness (K_D) equal to (E_{mo})·(*AREA1*)/(element length). The area of the section of the element is assumed to be dependent on the deformation, *AREA1* at displacement *R1*, and *AREA2* at displacemet *R2*. The shape of the envelope of the hysteretic cycles was assumed to be parabolic. The peak of the curve was defined by the point (ε'_m, f'_m) and the intersection with the x-axis occurs at the value of deformation ε_u. The slope of the descending branch of the curve was determined by the factor γ_{un}, while the reloading factor α_{re} defines the point at which the reloading curves attain the strength envelope. The closing strain, ε_{cl}, corresponds to the partial closing of the cracks where the compressive stresses could be developed.

The final parameters of the calibrated diagonal macro-elements, representig the innovative infill system, are listed in Table 5, both for the case of fully infill and infill with opening.

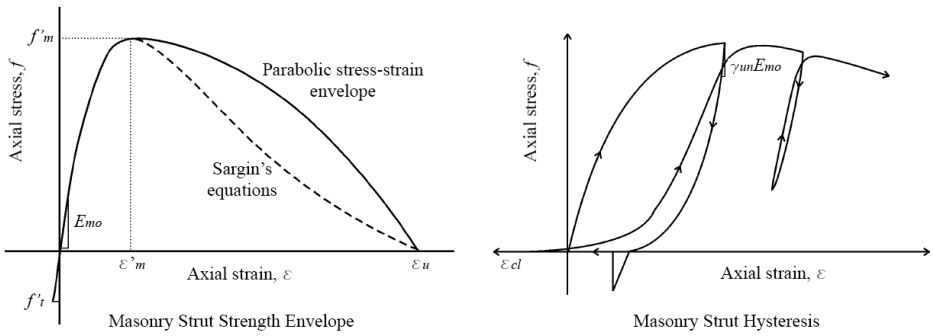

Figure 7: Masonry Strut Strength Envelope and Masonry Strut Hysteresis for Crisafulli rule [6].

Parameters of the element		Fully infill	Infill with opening	
K_D	kN/m	81371	54644	*initial diagonal stiffness*
f'_m	kPa	-1297	-1372	*compressive strength*
ε'_m	-	-0.00047	-0.0005	*strain at* f'_m
ε_u	-	-0.99	-0.99	*ultimate strain*
ε_{cl}	-	0.47	0.5	*closing strain*
E_{mo}	MPa	2967	2967	*initial masonry modulus*
γ_{un}	-	5	2	*stiffness unloading factor*
α_{re}	-	0.12	0.01	*strain reloading factor*
AREA1	m^2	0.1518	0.102	*initial strut cross-sectional area*
AREA2	m^2	0.1053	0.065	*final strut cross-sectional area*
R1	m	-0.0024	-0.0028	*displacement at 1*
R2	m	-0.0073	-0.028	*displacement at 2*

Table 5: Parameters of the diagonal struts.

Figure 8(a), Figure 8(b) and Figure 8(c) show the comparison, in terms of force-displacement curve, between the in-plane cyclic tests (black line) and the numerical models (red line) on the bare frames and on the frames infilled with the innovative system (with and without opening). Figure 8(d) also reports the comparison of the three envelope numerical curves. The input of the numerical-model was given by the loading history of the displacement effectively applied at the half-height of the top-beam during the pseudo-static cyclic tests. The plots show that the force-displacement curves of the numerical models match very well the experimental ones, during all the cycles.

In the cases of the infilled frames (both with and without opening), it was also possible to evaluate the energy dissipated during each cycle. Figure 9 shows the comparison between the energy dissipated by the frames during the in-plane cyclic tests and the one of the numerical models, which fit very well. Based on these results, it is possible to consider this macro-modeling approach accurate enough for the purpose of the present work.

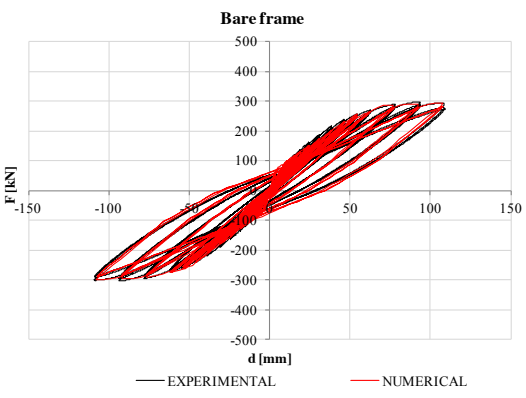

(a)

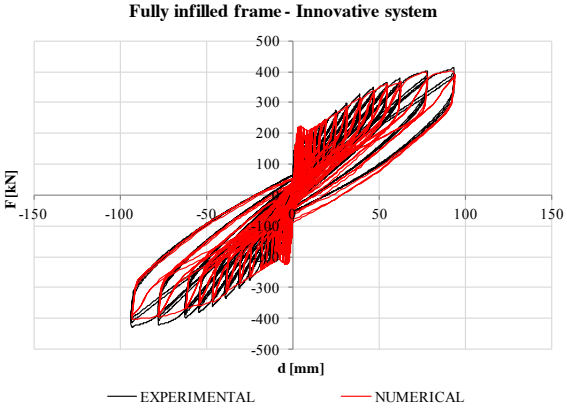

(b)

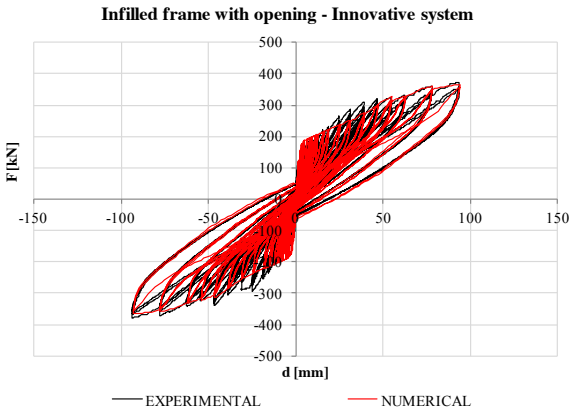

(c)

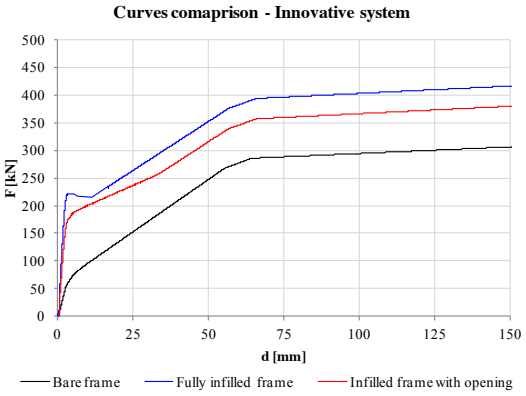

(d)

Figure 8: Comparison between the force-displacement experimental and numerical curves: (a) bare frame; (b) fully infilled case; (c) partially infilled case. (d) envelope comparison between the three calibrated models.

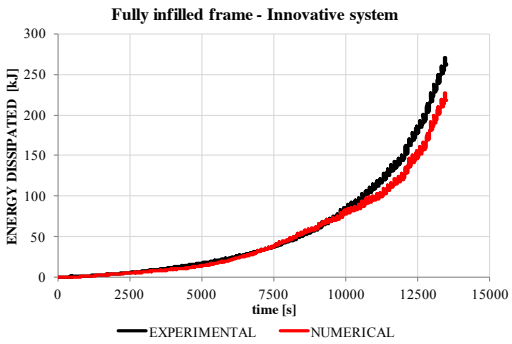

(a)

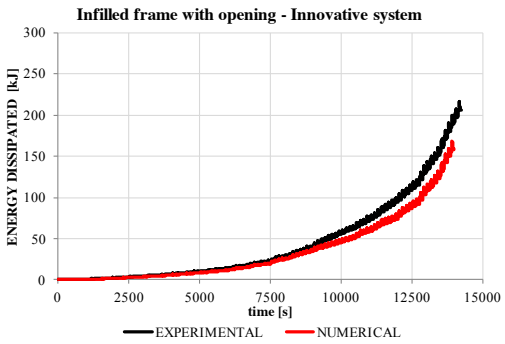

(b)

Figure 9: Comparison between the energy dissipation of the in-plane cyclic tests and the numerical models: (a) fully infilled case; (b) partially infilled case.

Moreover, in Figure 10(a), the macro-model hysteretic response of the double-leaf "traditional" infill (cyclic in-plane response and its envelope) is shown. The infill is modeled with two diagonal struts with the envelope and the hysteretic laws by Crisafulli ([15]), evaluating the stiffness and the strength with the criteria proposed by Decanini et al. ([17]), as indicated in Hak et al. in [7].

Figure 10(b) finally reports the comparison between the innovative systems and the traditional one in terms of the numerical infill contribution envelopes.

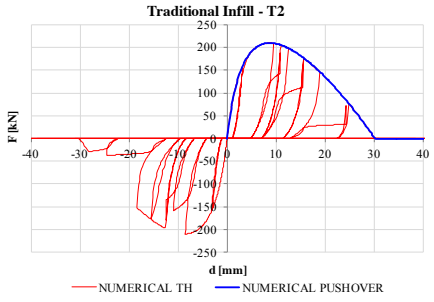

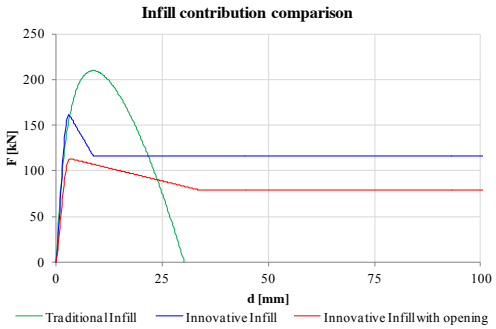

Figure 10: (a) Macro-model calibration of the double-leaf traditional infill (cyclic in-plane response and envelope); (b) envelope of the infill contributions between the innovative systems and the traditional one.

5 NON-LINEAR ANALYSES ON BARE AND INFILLED BUILDINGS

A series of non-linear static ("pushover") and dynamic time-history analyses have been performed on the case-study building, with different infill configurations, in order to evaluate the influence of the infills in the seismic response of the structures. A macro-modeling approach using the program Ruaumoko, as defined for the numerical calibration of the single infilled frames, was adopted. Three case-study frames were defined, one per each level of design PGA: 0.10g·S, 0.25g·S and 0.35g·S. In the case of the innovative infill solution with sliding joints, for each of the three case-study frames, five different configurations were considered, one bare and four infilled, as reported in Figure 11. In the case of the "traditional" infills, only two configurations have been taken into account: the partially infilled frame (Figure 11b) and the one side partially infilled frame (Figure 11d).

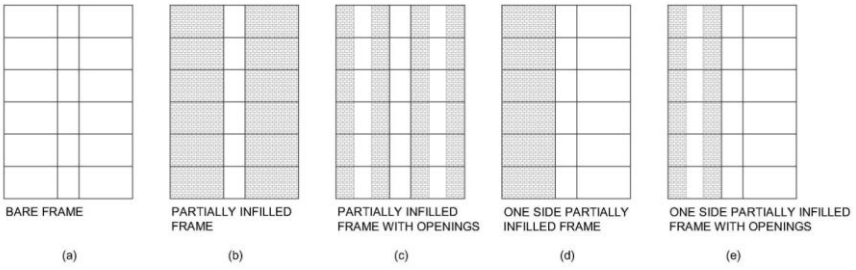

Figure 11: Different infilled configurations for the six-storey building.

As for the case of the simple portal-frame described before, the macro-modelling of the case-study frames was based on a concentrated-plasticity modeling approach (Figure 12a), where the RC beams and the columns were represented by Giberson elements and the behavior of the rotational springs at the RC member ends was assumed to be defined by the Takeda hysteresis rule [18] (Figure 12b), with no strength degradation. The stiffness corresponding to unloading and reloading is characterised through the definition of coefficients α and β ($\alpha = 0.5$ for both beams and columns; $\beta = 0.3$ for beams and $\beta = 0.0$ for columns), while the ratio between initial and post-yielding stiffness is defined by the Ramberg-Osgood moment-curvature bi-linear factor r ($r = 0.01$ for beams and columns) (Figure 12c). Also in this case, the possibility of shear failure occurrence in the structural elements is not considered, supposing the frames are properly designed and detailed according to modern seismic design code provisions. The gross stiffness of the RC structural members was reduced and the ratio of the effective to elastic initial stiffness was set equal to 0.25 for beams and 0.35 for columns. In the regions of intersection between beams and columns the, finite-length elastic elements were introduced. The viscous damping was represented by a tangent stiffness Rayleigh model. Following the recommendations by Priestley et al. ([13]) the damping corresponding to the fundamental mode of vibration was reduced and a value of 3.0% is adopted, while 5.0% damping was assumed in the second mode. The masses of the structure were lumped in the central nodes between the beams and the columns.

The models used for the infills are those evaluated in the calibration of the in-plane cyclic tests on the single storey-single bay infilled frames.

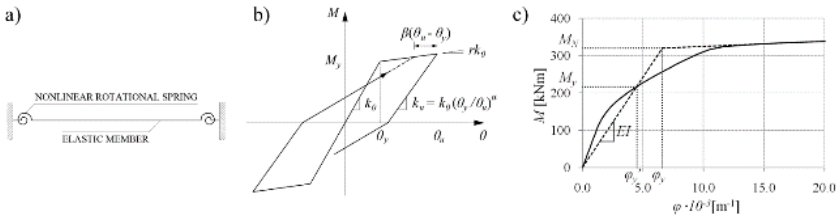

Figure 12: Concentrated-plasticity frame member; (b) Modified Takeda hysteretic rule; (c) Moment-curvature bilinear idealization.

5.1 Pushover analyses

In the non-linear static analyses, the horizontal action was given by means of equivalent horizontal loads applied at each mass of the structure. The intensity of the forces has increased monotonically, while their distribution was kept constant and proportional to the first modal shape of the structure. The capacity curves obtained from the pushover analyses (base shear vs roof displacement) on the configurations with the innovative infills are reported in Figure 13. On the capacity curves, the steps corresponding to the first attainment of the different limit states (OLS, DLS and LSS/ULS) in the first infill of the buildings with the drift capacity defined in Section 3, has been indicated.

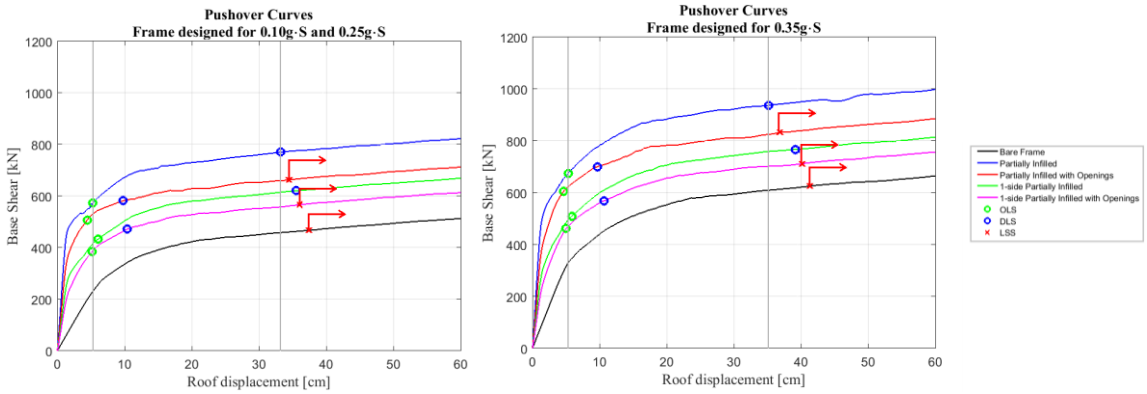

Figure 13: Capacity curves for the bare ad infilled (innovative system) frames.

For what concerns the buildings with the innovative infills, Figure 13 shows that no strength degradation on the capacity curve is found. The frame-models are therefore capable to attain large levels of displacements without reducing the base shear resistance. The shape and the trend of the curves are similar each other, and, as expected, the frame designed for higher level of PGA reach higher values of base shear. In addition, the curves of the infilled frames show higher values of base shear respect to the curves relative to the bare frame. In particular, the partially infilled frame system is the one capable to withstand higher level of horizontal forces. This difference is more evident in the initial part of the plot, in which also the stiffness reaches larger values. After the elastic range, the slope of the curves decreases and the curves keep themselves almost parallel to each other. The partially infilled frame reaches 3.0% of drift in correspondence of a value of roof displacement smaller than the others system. Moreover, it is possible to notice that the more the system is rigid and capable to withstand higher forces, the more the system shows smaller value of top displacement in correspondence of the same level of maximum inter-storey drift. In order to compare numerically in terms of resistance the different pushover curves, the base shear correspondent to the values of displacements related to the performance levels of the infill as reported in Section 3 was evaluated (see the gray vertical lines in Figure 13). Finally, it is interesting to notice that the

opening in the infill walls does not weaken the system significantly before the attainment of the OLS in comparison with the case without opening. The increase of base shear of the infilled structures is smaller for RC frames designed for higher seismic actions since the contribution of the infills in the global strength of the building affects to a lesser extent for more resistant and stiff RC structures.

A comparison in terms of the initial stiffness of the innovative system has also been performed, evaluating it as the secant stiffness at 50% of 0.6 times the base shear level reached at the life safety limit state (Figure 14). The reason of this choice is that, commonly, the bilinear idealization of a pushover curve pass through the point at $0.6 \cdot V_{max}$ (V_{max}: maximum value of base shear). The reduction of 50% is needed to catch the behavior of the system in the initial phase, in which the elements still behave elastically. The partially infilled frame system is the stiffest one and the partially infilled frame with opening is more rigid than the 1-side infilled frame. As expected, the presence of the infills increases the overall rigidity of the structure, compared to the bare frame configuration. It is interesting to note that the increase in stiffness of the infilled structures is smaller for RC frames designed for higher seismic actions since the contribution of the infills in the global stiffness of the building affects to a lesser extent for more resistant and stiff RC structures.

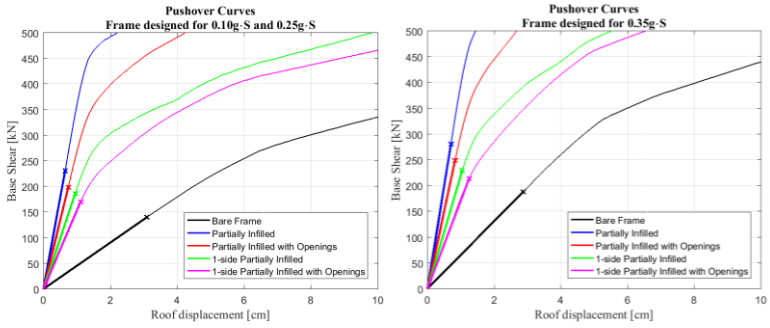

Figure 14: Initial part of the capacity curves for the bare and infilled frames with innovative infill.

Figure 15 shows the differences between the traditional and innovative infill systems, considering the infills in one side of the frame or in both sides, without taking into account the presence of an opening. The traditional system has a similar initial stiffness of the innovative one, but after the reaching of a peak in terms of base shear, a fast force degradation occurs until the attainment of a certain level of force that corresponds to the LSS (red dots); this limit is reached at very low level of roof-displacement respect to the innovative solution. At larger values of displacements, after the exceed of the ultimate conditions of the infills, the overall behavior of these structures tends to approximate (regardless by numerical instability) the response of the RC bare frames. On the other side, the buildings with the innovative infills do not show any strength degradation on the capacity curve and are able to attain much larger levels of displacement capacity before reducing the base shear resistance, as respect to the traditional ones.

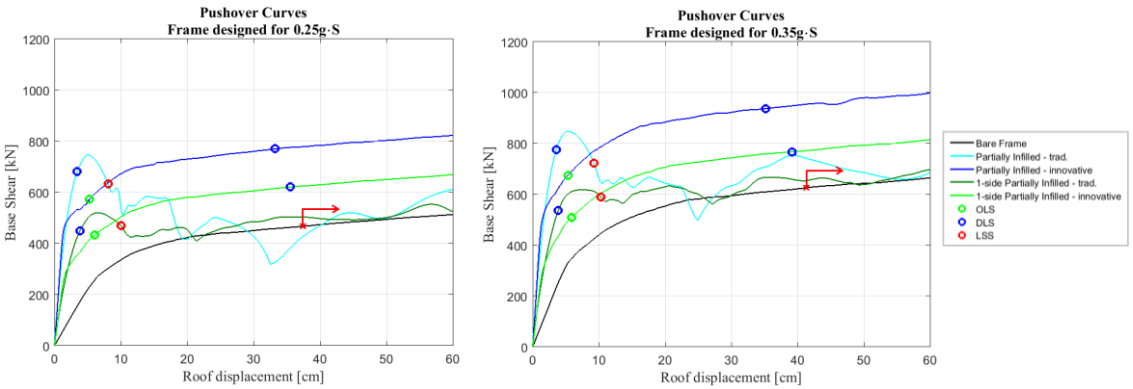

Figure 15: Capacity curves for the bare ad infilled (innovative and traditional systems) frames.

5.2 Non-linear dynamic analyses

Non-linear dynamic analyses were performed on each case-study frame for each configuration defined previously. The input ground motions were scaled to the DLS and to the ULS.

The selection of the earthquake records was done based on the recommendation of previous studies ([19]) on natural ground motions scaled to specified levels of seismicity. Ten earthquake input ground motions were considered per each group of analyses relative to a specific frame model, which is a number larger than the minimum number of seven records given by the European seismic codes ([10], [11]) to consider average response quantities from all the analyses. The software REXEL [20] was adopted to select the earthquakes from the European database. The average value of the ten records was matched with the target spectrum (±10%) in a range between $0.2 \cdot T_1$ and $2 \cdot T_1$, where T_1 is the fundamental period of the structure. The selected spectrum compatible records were scaled to the design value of PGA of the case-study frames. The records compatible to EC8 spectrum Type 1 are relative to the case-study frames designed for PGA equal to 0.25g·S and 0.35g·S, while the ground motions compatible to EC8 spectrum Type 2 are related to the case-study frames designed for PGA = 0.10g·S. In accordance with the design procedure, to obtain records compatible with the spectrum corresponding to the damage limitation limit state, the reduction factor $\nu = 0.5$ was applied. Only earthquakes recorded on soil class B are considered, with magnitudes between 5.5 and 8.0 for Type 1 and between 3.5 and 5.5 for Type 2 spectra. In Figure 16, the spectrum compatible earthquake records at the ULS with PGA equal to 0.10g·S and 0.25g·S have been reported.

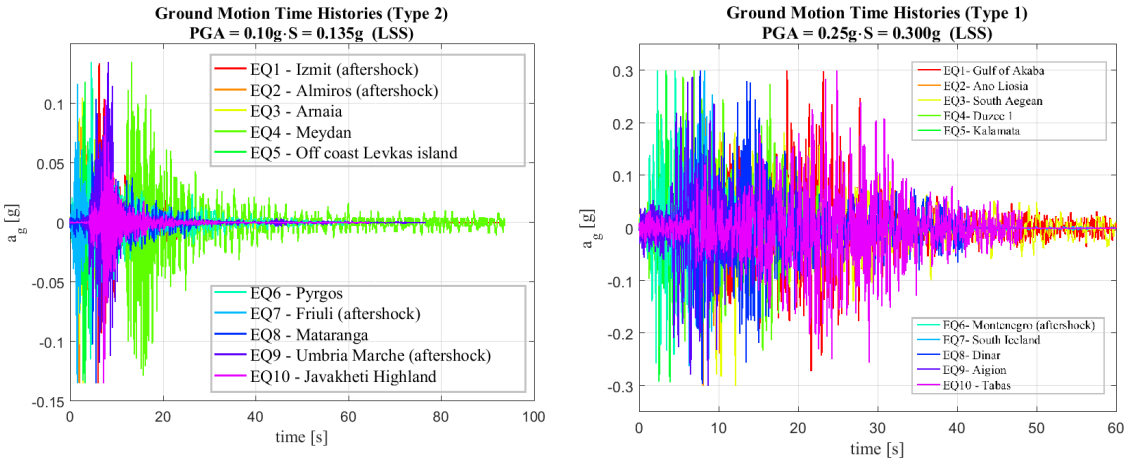

Figure 16: Design spectrum compatible earthquake records at the ULS: (a) PGA=0.10g·S; (b) PGA=0.25g·S.

The floor displacements and inter-storey drifts coming from the dynamic non-linear analyses have been evaluated. The selection of the input ground motion has a great influence in the response on the structures, also considering that different frame typologies, both infilled and bare, with different modes of vibrations, behave differently to the same earthquake. Nevertheless, considering that the sets of input ground motion adopted in the analyses were composed by ten spectrum compatible accelerograms, the quantities related to the response of the structure were analyzed in terms of average values. The following figures (from Figure 17 to Figure 20) summarize the displacement and drift profiles for each set of accelerograms, considering the bare frames, the four configurations with the innovative infills and the two with the traditional infills. Displacement profiles are obtained for each frame type and for each ground motion record corresponding to the instant of a maximum displacements obtained in any of the storeys. The lines in the displacement-plots (Figure 17 and Figure 18) represent the average values of the displacement for the specific set of accelerograms. Drift profiles are obtained for each frame type and for each ground motion record corresponding to the instant of a maximum drift obtained in any of the storeys. The lines in the drift-plots (Figure 19 and Figure 20) represent the average values of the maximum drifts for the specific set of accelerograms.

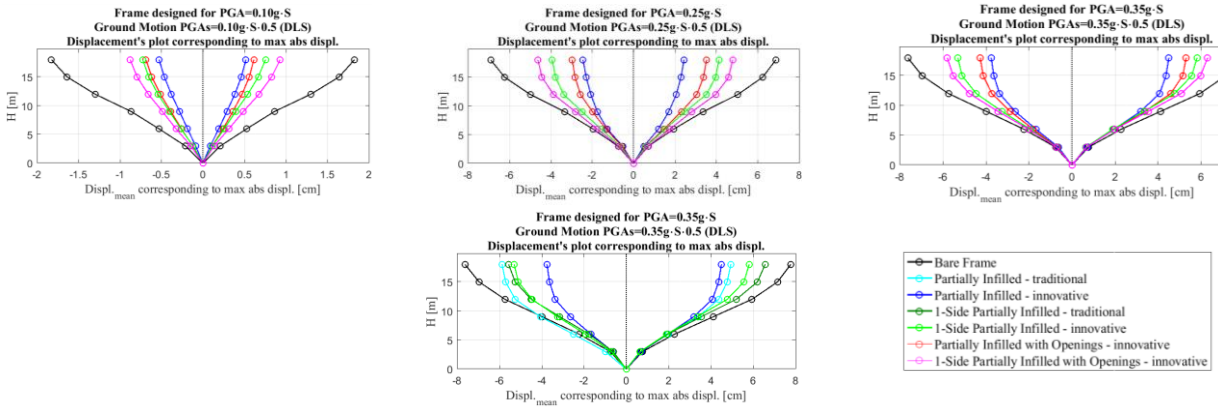

Figure 17: Displacement profiles at the DLS.

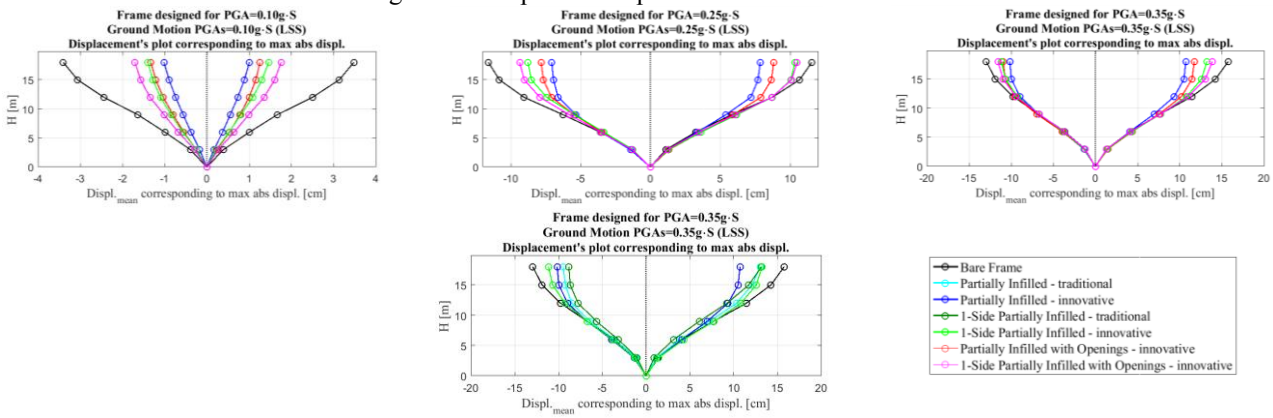

Figure 18: Displacement profiles at the LSS (ULS)

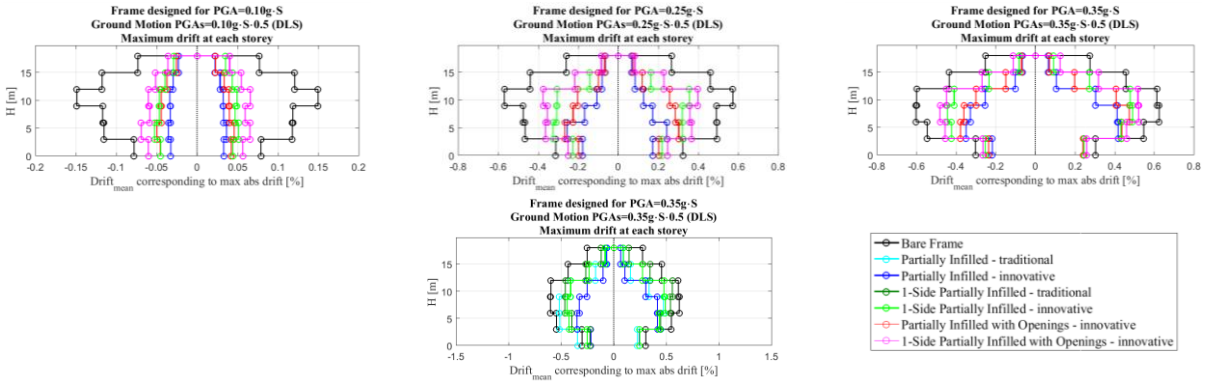

Figure 19: Inter-storey drift profiles at DLS.

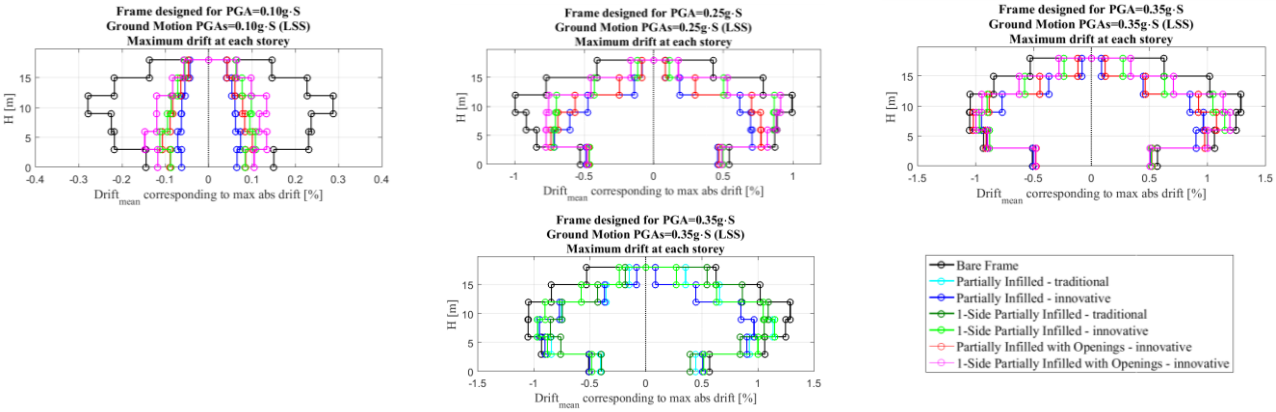

Figure 20: Inter-storey drift profiles at LSS (ULS).

Looking at the response in terms of displacements of the structures (Figure 17 and Figure 18), it is possible to notice that the maximum absolute displacement is always the one relative to the upper floor and therefore no higher mode of vibrations occur; the displacement shapes relative to the achievement of the maximum displacement is almost the same for all the configurations (approximately linear with the exception of the upper floors).

As expected, the presence of the infills (both the innovative and traditional ones) in the frames reduces considerably the maximum value of displacement demand as respect to the bare structures and, in particular, the partially infilled frames configuration exhibits the lowest values of displacements.

Another series of considerations can be done looking at the drift profiles (Figure 19 and Figure 20). Besides the fact that the drift demands are larger for the bare frames than for the infilled configurations, the drift profile of the frames without infills is quite different from the configurations with walls. Moreover, it is possible to notice that the maximum drift for the bare frame configuration is reached in correspondence of the fourth storey, while in the other cases it is located between the second and the third floor. In some cases, the buildings with traditional infills have reached higher drift demands respect to the ones with innovative infills due to their brittle behavior having a sharp descending branch after the peak force and, therefore, providing a smaller contribution to the overall in-plane response of the buildings that lead to a performance more similar to the one of a bare frame.

Comparing the three different structures designed for the three levels of PGA, the difference in terms of drifts and displacements between the bare frame and infilled frames configurations diminish with the increase of PGA level. This effect was expected since the properties of the infills remain the same while the sections of beams and columns change.

Furthermore, for all the cases considered, from observations on the displacement and drift profiles, no occurrence of any soft-storey mechanisms appears.

In the case of traditional infills, the reduction of drift demands appears to be more significant at DLS than at ULS, due to the fact that, subjected to the design seismic action at ULS, the traditional are severely damage, as better specified in the following section.

Interestingly, the results also illustrate that, at the DLS, storey drifts for the bare frames in some cases exceed the design limit of 0.5%, suggesting that the current code approach is unable to fully control the response of traditional infills rigidly attached to the structure. The fact that drifts are larger than expected can be attributed in part to the EC8 recommendation to use 50% of the gross section flexural and shear stiffness for the section stiffness when in fact the cracked section stiffness is often lower, and in part to the fact that the frames enter into the inelastic response range also under the DLS seismic action, and consequently the displacements are higher than predicted by a linear analysis with initial stiffness.

6 SEISMIC PERFORMANCE OF THE INFILLED BUILDINGS

The distribution of in-plane damage due to the action of selected earthquake records is evaluated from the results of dynamic non-linear analyses for each considered frame type and infill typology at the different limit states. The damage of a single infill is assessed through the maximum achieved drift. In particular, the frames are assumed to fulfil the performance criteria if the requirements defined in Table 6 are satisfied for more than 50% of the earthquake records (at least 6 out of 10).

	Fully infill with sliding joints	**Infill with sliding joints with opening**	**Traditional Infill - Double leaf T2**
	$Drift_{\_max\_storey\_i} < 0.5\%$ (OLS)	$Drift_{\_max\_storey\_i} < 0.4\%$ (OLS)	$Drift_{\_max\_storey\_i} < 0.2\%$ (OLS)
	$0.5\% \leq Drift_{\_max\_storey\_i} < 3.0\%$ (DLS)	$0.4\% \leq Drift_{\_max\_storey\_i} < 0.9\%$ (DLS)	$0.2\% \leq Drift_{\_max\_storey\_i} < 0.3\%$ (DLS)
	$Drift_{\_max\_storey\_i} \leq 3.0\%$ (LSS=ULS)	$0.9\% \leq Drift_{\_max\_storey\_i} \leq 3.0\%$ (LSS=ULS)	$0.3\% \leq Drift_{\_max\_storey\_i} \leq 1.0\%$ (LSS=ULS)
	$Drift_{\_max\_storey\_i} > 3.0\%$	$Drift_{\_max\_storey\_i} > 3.0\%$	$Drift_{\_max\_storey\_i} > 1.0\%$

Table 6: Performance levels of the infills ([4], [7]).

From Figure 21 to Figure 22, the in-plane damage distribution obtained for each configuration of the infilled frames designed for PGA=0.35g·S is displayed. The colors of the infills indicate if a certain limit state is exceeded or not according to the procedure of Table 6.

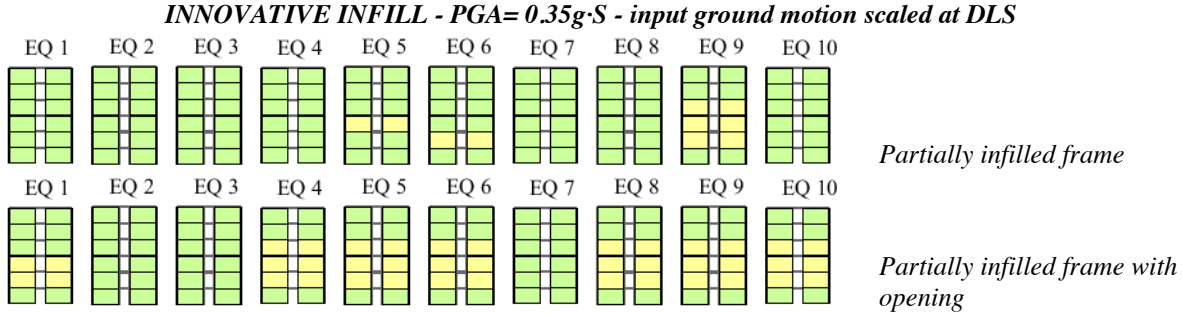

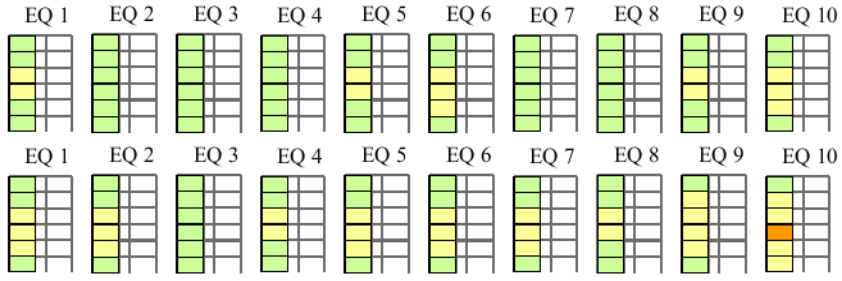

Figure 21: Damage distribution of dynamic analyses of infilled frame designed for PGA=0.35g·S and subjected to the input ground motions scaled to DLS: PGA=0.35g·S·0.5.

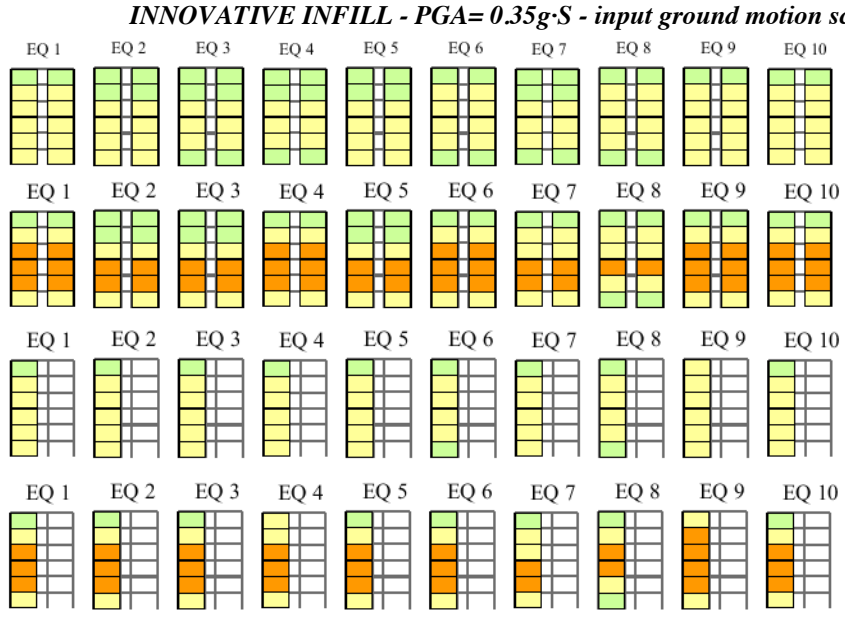

Figure 22: Damage distribution of dynamic analyses of infilled frame designed for PGA=0.35g·S and subjected to the input ground motions scaled to LSS: PGA=0.35g·S.

All the configurations with the innovative infills largely satisfy the performance criteria at ULS and DLS for all the applied levels of PGA (the largest value applied was 0.35·S g).

In particular, the drift limits related to the life safety limit state (LSS/ULS) are never exceeded in any of the infill configuration and frame typology. In the case of frames designed for a PGA=0.10·S g, no input ground motion set, even if it is scaled to its relative ULS, has caused the exceeding of OLS. In the case of frame designed for a PGA=0.25·S g, if the input ground motions are scaled to the DLS, the DLS drift limit is never achieved. If the input accelerograms are scaled to the LSS, the DLS is exceeded in some cases, but only in the configurations in which the infills have the opening. In the case of frames designed for a PGA=0.35·S g, if the ground motions are scaled to the DLS, only one of the one-side infilled frames with the openings exceeds the drift limit at the DLS. In case of accelerograms scaled to LSS, the drift at DLS is achieved by the frame models with the infills with the openings but, on the other hand, the frames with the infills without openings never reach this limit.

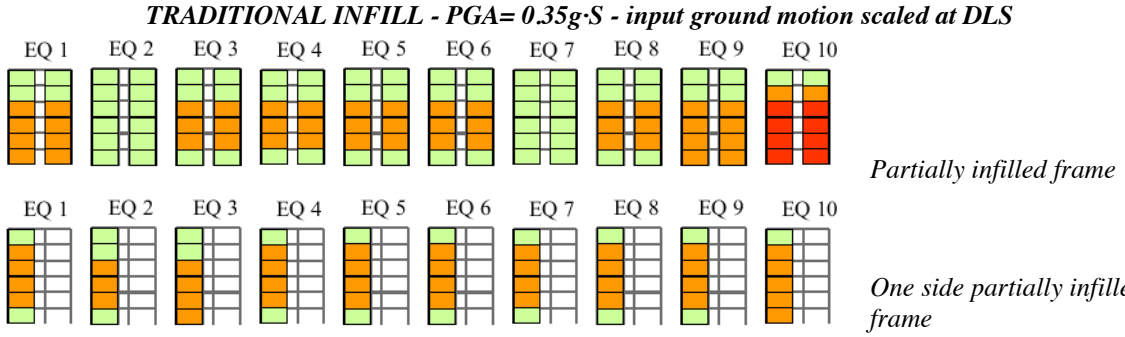

Figure 23: Damage distribution of dynamic analyses of traditional infilled frame designed for PGA=0.35g·S and subjected to the input ground motions scaled to DLS: PGA=0.35g·S·0.5.

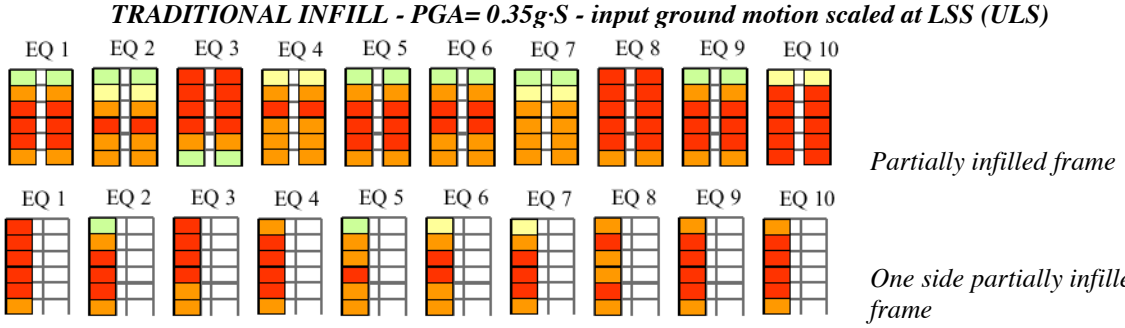

Figure 24: Damage distribution of dynamic analyses of traditional infilled frame designed for PGA=0.35g·S and subjected to the input ground motions scaled to LSS: PGA=0.35g·S.

The traditional infills, for both configurations that have been taken into account, show a lower seismic performance respect to the innovative system. The values of drifts at DLS and at ULS reported in Table 6 have been always exceeded for ground motions scaled at DLS and ULS, respectively. Therefore, considering the analyses performed within the case studies taken into account, the respect of the limit states is never fulfilled, due to the fact that the drift limitations of the bare frame imposed by the standards at the design levels are not safe-sided for the traditional infills, as concluded by Hak et al in [7].

7 CONCLUSIONS

Within the European FP7 Project "INSYSME" ([5]) the research unit of the University of Pavia has conceived a new seismic resistant masonry infill ([1], [2]), with sliding joints within the wall and deformable joints at the panel/frame interface which, through an extensive experimental campaign, has showed a strong reduction of the level of damage respect to the traditional completely adherent solutions.

The present work has been focused on the in-plane seismic performance of the innovative infill and its influence in the overall in-plane behaviour of RC buildings. The in-plane seismic behaviour of the innovative infills (with and without opening) has been calibrated on in-plane cyclic tests ([3], [4]) by modelling the infill with macro-elements composed by two diagonal non-linear struts pinned at two edges according to the Crisafulli hysteretic rule ([15]).

RC frame buildings have been designed to three different PGA levels and various infill configurations have been taken into account in order to perform 2D nonlinear static and dynamic analyses on several distinct case studies. Moreover, considering the results on a previous research ([7]), a comparison with the results with traditional double leaf masonry infills

has been conducted. Focusing on parameters such as the displacement profile, the inter-storey drift and the base shear, the overall in-plane seismic response of the buildings has been discussed as a function of the infill type and configuration, also in comparison with the bare frame case.

As expected, the presence of the infills modifies the global behaviour of the structure, and the differences to the bare frame configuration are more pronounced in the case of buildings designed for lower levels of PGA and infilled with the traditional system.

The buildings with the innovative infills have always widely satisfied the “life safety” (ULS), the “damage limitation” (DLS) and the “operational” performance limit states both for the case of the infill with and without opening. In the case of the infilled configurations without opening, no analyses have ever even reached any inter-storey drift limit at ULS and DLS in any storey with ground motions scaled at ULS and DLS, respectively. Therefore, based on these results applied on the considered case studies, it is possible to infer that the performance of the infill system with sliding joints proposed by the University of Pavia is excellent at any limit state (OLS, DLS and ULS) with the applied seismic actions.

The results also exhibit a significant improvement of the in-plane performance compared to a commonly adopted “traditional” infill system constituted by a double leaf wall of a horizontally perforated clay unit masonry.

This research is only a first step for a full understanding of the overall in-plane seismic behaviour of RC buildings infilled with the innovative solution and further numerical investigation should be performed in order to carry out a larger number of non-linear time-history analyses applied to a wider range of PGA levels and structural configurations with different infill distribution.

AKNOLEDGEMENTS

This study has been carried out the University of Pavia and EUCENTRE within the project INSYSME "Innovative Systems for earthquake resistant Masonry Enclosures in rc buildings", grant FP7-SME-2013-2-GA606229, 2013-2016 and the Executive Project DPC-RELUIS 2010-2013. The financial support received is gratefully acknowledged.

REFERENCES

[1] P. Morandi, R.R. Milanesi, G. Magenes, Soluzione innovativa per tamponatura antisismica in laterizio a giunti scorrevoli [in Italian], *XVI ANIDIS,* L'Aquila, Italy, September 13-17, 2015.

[2] P. Morandi, R.R. Milanesi, G. Magenes, Innovative seismic solution for clay masonry infills with sliding joints: principles and details, *16th IBMAC*, Padova, Italy, June 26-30, 2016.

[3] R.R. Milanesi, P. Morandi, G. Magenes, Innovative seismic solution for clay masonry infills with sliding joints: experimental tests, *16th IBMAC*, Padova, Italy, June 26-30, 2016.

[4] P. Morandi, R.R. Milanesi, C.F. Manzini, G. Magenes, Experimental tests of an engineered seismic solution of masonry infills with sliding joints, *16th WCEE,* Santiago de Chile, Chile, January 9-13, 2017.

[5] INSYSME "Innovative Systems for earthquake resistant Masonry Enclosures in RC building", European project, grant FP7-SME-2913-2-GA606229, 2013-2016.

[6] A.J. Carr, Ruaumoko Manual, University of Canterbury, Cristchurch, New Zealand, 2007.

[7] S. Hak, P. Morandi, G. Magenes, T. Sullivan, Damage control for clay masonry infills in the design of RC frame structures, *Journal of Earthquake Engineering,* vol. 16, S1, pp. 1-35, 2012.

[8] G.M. Calvi, D. Bolognini, Seismic response of RC frames infilled with weakly reinforced masonry panels, *Journal of Earthquake Engineering*, Vol. 5, No. 2, pp. 153-185, 2001.

[9] CEN *Eurocode 2 - Design of concrete structures, Part 1-1: General rules and rules for buildings,* European Committee for Standardisation, ENV 1992-1-1, Brussels, Belgium, 2004.

[10] CEN *Eurocode 8 - Design of structures for earthquake resistance*, *Part 1: General rules, seismic actions and rules for buildings*, EN 1998-1, European Committee for Standardisation, Brussels, Belgium, 2004.

[11] NTC08 *Norme Tecniche per le costrutioni* (in Italian), Ministero delle Infrastrutture e dei Trasporti, Roma : Decreto Ministeriale of 14th January 2008, 2008

[12] M.F. Giberson, The response of nonlinear multi-story structures subjected to earthquake excitation, *EERL Report*, California Institute of Technology, Pasadena, California, 1967.

[13] Priestley, M.J.N., Calvi, G.M., and Kowalsky, M.J., Displacement-Based Seismic Design of Structures, *IUSS Press*, Pavia, Italy, 2007.

[14] Y. Fukada, Study on the restoring force characteristics of reinforced concrete buildings *[in Japanese], Proceedings Kanto District Symposium*, Architectural Institute of Japan, Tokyo, Japan, No. 40, 1969.

[15] F.J., Crisafulli, Seismic behaviour of reinforced concrete structures with masonry infills, *PhD Dissertation*, Department of Civil Engineering, University of Canterbury, New Zealand, 1997.

[16] R.R. Milanesi, Seismic performance of a newly conceived masonry infill with sliding joints, *PhD Dissertation*, UMESchool, University of Advanced Studies IUSS Pavia, Italy, 2016.

[17] L. Decanini, F. Mollaioli, A. Mura, R. Saragoni, Seismic performance of masonry infilled RC frames, *Proceedings of the 13th World Conference of Earthquake Engineering,* Vancouver, Canada, 2004.

[18] S. Otani, Nonlinear dynamic analysis of reinforced concrete building structures, *Canadian Journal of Civil Engineering,* Vol. 7, pp. 333-344, 1980

[19] I. Iervolino, G. Maddaloni, E. Cosenza, Eurocode 8 complian real record sets for seismic analysis of structures, *Journal of Earthquake Engineering,* Vol. 12, pp. 54-90, 2008.

[20] I. Iervolino, C. Galasso, E. Cosenza, REXEL: computer aided record selection for code-based seismic structural analysis, *Bulletin of Earthquake Engineering*, Vol. 8, pp. 339-362, 2010.